compete with the σ,σ^* fluorescence. It should be either that the σ,σ^* fluorescence is extremely fast or that the above radiationless process is extremely slow. In order to examine this, we try to determine the radiative rate constant for the σ,σ^* fluorescence from the absorptivity of the reverse transition. In evaluating the ϵ value from the observed absorptivity, we assume that the molecular weight of the polymer is uniformly 1.2×10^5 (peak value in Figure 1). With this assumption, ϵ at the peak of the absorption ($\sim$340 nm) is determined as 8.7×10^6 cm^{-1} M^{-1}. The radiative rate constant for the reverse emission is then determined as 5×10^{10} s^{-1}. It has thus been clarified that the σ,σ^* fluorescence is a significantly fast process; it can easily compete with the radiationless transition to the σ,π^* state. Large absorptivity found for the transition to the σ,σ^* state and hence the high emissivity of the σ,σ^* emission is understood also theoretically in view of the large density of state at the bottom of the σ^* conduction band as is seen in Takeda et al.[18]

The source of the temperature dependence observed for the broad band is not quite understood at this moment. A decrease of fluorescence or phosphorescence intensity at higher temperature is quite commonly observed for many organic molecules and is usually interpreted in terms of the existence of a fast decaying electronic or vibronic state. However, such a significant temperature dependence of the intensity at such a low-temperature region is not so common. The discussion of this subject therefore has to be postponed until the experiments on the temperature dependence of the lifetime are completed.

Acknowledgment. We thank Professor H. Sakurai, Dr. K. Sakamoto, and K. Obata for their fruitful discussions and guidance in the synthesis of the polymer. Gel permeation fractionation was kindly performed by Dr. S. Ito of Kyoto University, to whom we express our appreciation. The present paper was supported in part by Grant-in-Aid for Scientific Research (No. 62430001 and No. 62213003) from the Ministry of Education, Science and Culture.

Registry No. Poly(methylphenylsilylene) (homopolymer), 31324-77-3; poly(methylphenylsilylene) (SRU), 76188-55-1.

References and Notes

(1) Kagawa, T.; Fujino, M.; Takeda, K.; Matsumoto, N. *Solid State Commun.* **1986**, *57*, 635.
(2) Harrah, L. A.; Zeigler, J. M. *J. Polym. Sci. C* **1987**, *25*, 205.
(3) West, R. *J. Organomet. Chem.* **1986**, *300*, 327.
(4) Terazima, M.; Ito, O.; Yamazaki, I.; Tamai, N.; Azumi, T., unpublished results.
(5) Yanari, S. S.; Bovey, F. A.; Lumry, R. *Nature (London)* **1963**, *200*, 242.
(6) Basile, L. J. *J. Chem. Phys.* **1962**, *36*, 2204.
(7) Nishijima, Y. *J. Polym. Sci. C* **1970**, *31*, 353.
(8) Torkelson, J. M.; Liptay, S.; Tirrell, M. *Macromolecules* **1981**, *14*, 1601.
(9) Ito, S.; Yamamoto, M.; Nishijima, Y. *Bull. Chem. Soc. Jpn.* **1981**, *54*, 35.
(10) Todesco, R. V.; Kamat, P. V. *Macromolecules* **1986**, *196*, 796.
(11) David, C.; Lempereur, M.; Geuskens, G. *Eur. Polym. J.* **1973**, *9*, 1315.
(12) Vala, M. T., Jr.; Haebig, J.; Rice, S. A. *J. Chem. Phys.* **1965**, *43*, 886.
(13) David, C.; Piens, M.; Geuskens, G. *Eur. Polym. J.* **1972**, *8*, 1291.
(14) David, C.; Piens, M.; Geuskens, G. *Eur. Polym. J.* **1972**, *8*, 1019.
(15) Birks, J. B.; Lumb, M. D.; Munro, I. H. *Proc. R. Soc. London* **1964**, *A280*, 289.
(16) Azumi, T.; McGlynn, S. P. *J. Chem. Phys.* **1964**, *41*, 3131.
(17) Shizuka, H.; Sato, Y.; Ishikawa, M.; Kumada, M. *J. Chem. Soc., Chem. Commun.* **1982**, 439.
(18) Takeda, K.; Teramae, H.; Matsumoto, N. *J. Am. Chem. Soc.* **1986**, *108*, 8186.
(19) Rotkiewicz, K.; Grellmann, K. H.; Grabowski, Z. R. *Chem. Phys. Lett.* **1973**, *19*, 315; **1973**, *21*, 212.
(20) Rettig, W. *Angew. Chem. Int. Ed. Engl.* **1986**, *25*, 971.

Fluorescence Probes for Evaluating Chain Solvation in Network Polymers. An Analysis of the Solvatochromic Shift of the Dansyl Probe in Macroporous Styrene–Divinylbenzene and Styrene–Diisopropenylbenzene Copolymers

K. J. Shea,* D. Y. Sasaki, and G. J. Stoddard

Department of Chemistry, University of California, Irvine, Irvine, California 92717.
Received April 8, 1988; Revised Manuscript Received June 21, 1988

ABSTRACT: The wavelength of the fluorescence emission of dansyl probe 1 in pure organic solvent is red shifted as the solvent polarity, hydrogen bond donor ability, and hydrogen bond acceptor ability are increased. A variety of network polymers "doped" with 1 have been synthesized. An analysis of the solvatochromic shift of the fluorescence emission of these materials when imbibed in solvents has been found to correlate with the facility with which solvents penetrate the gel or continuous phase of these materials. The analysis is accomplished by comparisons of the fluorescence emission of 1 in dry polymer with that of the solvent-imbibed polymer. As expected, solvent penetrability decreases with increasing cross-linking density and is significantly influenced by the morphology of the material. The gel phase of macroporous resins can be significantly more penetrable than nonporous "beads" of comparable cross-linking. The nature of the porogen is found to exert a profound effect on the penetrability of macroporous materials. Support for the interpretation of the solvatochromic results is obtained from hydrolysis studies of bisketal templates that were incorporated into the matrix of the polymers by copolymerization. The hydrolysis yields in both tetrahydrofuran and methanol increase with increased solvent penetrability as revealed by the solvatochromic shift. The hydrolysis results in tetrahydrofuran are also paralleled by swelling studies; thus, a large volume increase in THF is paralleled by a high hydrolysis yield (THF/H_2O). The swelling ratio in methanol, however, does not correlate with hydrolysis yield. The probe technique permits survey of a variety of complex materials of widely different morphology.

Introduction

The facility with which solvents may penetrate the gel phase of a network polymer is an issue of fundamental importance,[1,2] and diagnositics have been employed to evaluate this phenomenon.[3] Network polymers of complex morphology, such as macroporous resins,[4] pose particularly

0024-9297/89/2222-1722$01.50/0

Table I
Suspension Polymerization

	reaction mixtures							
polymer[a]	DVB, %	DVB, g	styrene, g	H_2O, mL	AIBN, mg	toluene, mL	probe 1, 10^3 g	Methocel, mg
DVB-50-S-T	50	20.0	0	200	200	20.0	5.66	100
DVB-50-S-N	50	20.0	0	200	200	0	5.66	90
DVB-20-S-T	20	9.00	11.0	200	200	20.0	6.45	100
DVB-20-S-N	20	9.00	11.0	200	200	0	6.45	70
DVB-5-S-T	5	2.40	17.6	200	200	20.0	6.88	100
DVB-5-S-N	5	2.40	17.6	200	200	0	6.88	80

[a] Polymer code refers to cross-linking monomer (DIP = diisopropenylbenzene, DVB = divinylbenzene)-% cross-linker in monomer mixture-type of polymerization (B = bulk, S = suspension)-porogen (T = toluene, A = acetonitrile, N = no porogen).

interesting challenges since solvent uptake and volume increase measurements may be complicated by the permanent porosity associated with these materials. Furthermore, the presence of microdomains with limited solvent access may limit the value of available techniques. We desired a simple diagnostic that would provide information regarding polymer chain solvation and/or penetrability of solvents in these complex materials. The success with which fluorescence probes have been utilized to report on the microenvironment, particularly in complex biological macromolecules,[5] warranted our consideration of this technique for the problem at hand.

In this paper, we report fluorescence studies of a Dansyl probe that is covalently incorporated into highly cross-linked macroporous network polymers by copolymerization.[6] An analysis of the wavelength of fluorescence emission of polymer particles imbibed in various solvents is found to correlate with the facility with which solvents *penetrate* the gel phase and solvate the polymer chains. The fluorescence results are compared with those obtained by using more conventional techniques such as solvent swelling. Furthermore, it was anticipated that solvation of the gel phase of network polymers would be related to the facility with which chemical reactions take place in the continuous phase. Indeed, a qualitative correspondence between gel solvation, as revealed by the probe technique, and a hydrolysis reaction of groups covalently bound in the gel phase has also been established. The probe method allows for the rapid survey of complex macroporous networks and permits one to readily evaluate the influence of porogen, the degree of cross-linking, and the nature of the cross-linking monomer on solvent penetrability of the network. In a later paper, the diffusion of electrophiles is found to correlate with the solvatochromic shift data.[7]

Experimental Section

All reactions were conducted in oven-dried (160 °C) glassware under positive N_2 atmosphere. All solvents were purified prior to use: ether and benzene were refluxed with sodium benzophenone and distilled, dimethylformamide was dried over 4-Å molecular sieves and distilled, and triethylamine was refluxed over calcium hydride and distilled. Methanesulfonyl chloride (Aldrich Co.) was distilled. Lithium aluminum hydride was used without further purification. The silica gel used for columns was of the 230–400-mesh grade (ICN Co.).

***p*-Vinylbenzyl Alcohol.** To a stirred solution of lithium aluminum hydride (0.195 g, 5.14 mmol) in dry diethyl ether (20 mL) was added a solution of *p*-vinylbenzoic acid[8] (0.500 g, 3.37 mmol) in dry Et_2O (10 mL) by syringe at a rate such that gentle reflux was maintained. After addition, the mixture was brought to reflux for 1.25 h. The solution was then cooled in an ice bath and quenched with consecutive portions of 0.2 mL of H_2O, 0.2 mL of 10% aqeuous sodium hydroxide, and 0.6 mL of H_2O. The organics were then dried over anhydrous magnesium sulfate, filtered, and evaporated in vacuo to yield the alcohol as a clear, colorless liquid (0.413 g, 91.2%). ^{1}H NMR δ 7.40 (d, J = 8.1 Hz, 2 H, ArH), 7.31 (d, J = 8.1 Hz, 2 H, ArH), 6.71 (dd, J = 10.9, 17.6 Hz, 1 H, CH=), 5.74 (d, J = 17.6 Hz, 1 H, =CH), 5.24 (d, J = 10.9 Hz, =CH), 4.66 (br d, J = 5.3 Hz, 2 H, CH_2O), 1.80 (br t, J = 5.3 Hz, OH); IR (neat) 3332 (br), 3088, 2874, 1630, 1512, 1407, 1031, 1013, 991, 908, 848, 824 cm^{-1}.

***p*-Vinylbenzyl Azide.** A dimethylformamide (10 mL) solution of sodium azide (0.400 g, 6.16 mmol), *p*-vinylbenzyl alcohol (0.413 g, 3.08 mmol), and triethylamine (0.86 mL, 6.2 mmol) was stirred at 0 °C for 20 min. Methanesulfonyl chloride (0.48 mL, 6.2 mmol) was syringed dropwise to the mixture and the temperature was maintained at 0 °C for 2 h and then allowed to slowly warm to room temperature. After 10 h, the solution was diluted with 20 mL of H_2O and 10 mL of aqueous saturated sodium chlroide solution and then extracted with diethyl ether (3 × 40 mL). The organics were combined and washed in aqueous HCl (50 mL), aqueous saturated sodium bicarbonate solution (50 mL), and aqueous saturated sodium chloride solution. The organics were dried over anhydrous magnesium sulfate and then filtered and evaporated in vacuo to a concentrated solution of ~2 mL. The concentrate was passed through a column of silica gel with eluent of 5% diethyl ether/hexanes, and the appropriate fractions were combined and evaporated in vacuo to yield vinylbenzyl azide (0.406 g, 82.8%) as a clear, colorless liquid. ^{1}H NMR δ 7.42 (d, J = 8.0 Hz, 2 H, ArH), 7.27 (d, J = 8.0 Hz, 2 H, ArH), 6.72 (dd, J = 17.6, 10.9 Hz, 1 H, CH=), 5.77 (d, J = 17.6 Hz, 1 H, =CH), 5.27 (d, J = 10.9 Hz, 1 H, =CH), 4.32 (s, 2 H, CH_2N); ^{13}C NMR δ 137.97, 135.08, 128.64, 126.89, 114.65, 102.01, 54.82; IR (neat) 3000, 2920, 2880, 2080, 1630, 1510, 1410, 1340, 1250, 990, 910 cm^{-1}.

***p*-Vinylbenzylamine.** Lithium aluminum hydride (50.0 mg, 1.28 mmol) in dry diethyl ether (14 mL) was stirred mechanically, and into it was syringed a solution of *p*-vinylbenzyl azide (0.406 g, 2.55 mmol) in dry diethyl ether (6 mL) in a dropwise manner. The mixture was stirred for 1 h at room temperature. The solution was cooled to 0 °C and then quenched with successive portions of 0.05 mL of H_2O, 0.05 mL of 10% aqueous sodium hydroxide, and 0.15 mL of H_2O and stirred for 0.5 h. The mixture was dried over anhydrous magnesium sulfate, filtrated, and evaporated in vacuo to yield the amine as a clear, slightly greenish yellow liquid (309 mg, 91.0%). ^{1}H NMR δ 7.39 (d, J = 8.0 Hz, 2 H, ArH), 7.27 (d, J = 8.0 Hz, 2 H, ArH), 6.71 (dd, J = 17.6, 10.9 Hz, 1 H, CD=), 5.73 (d, J = 17.6 Hz, 1 H, =CH), 5.22 (d, J = 10.9 Hz, 1 H, =CH), 3.85 (s, 2 H, CH_2N), 1.65 (br s, 2 H, NH_2); IR (neat) 3370, 3300, 3080, 3000, 2910, 2850, 1630, 1510, 1400, 990, 900, 820 cm^{-1}.

Dansyl Chloride. The chloride was generated by the method of Mendel.[9]

Dansyl Probe (1). Dansyl chloride (0.315 g, 1.17 mmol) was dissolved in a solution of benzene (10 mL) and triethylamine (0.5 mL, 3.15 mmol). *p*-Vinylbenzylamine (0.282 g, 2.12 mmol) was then added, and the mixture was stirred at room temperature for 12 h. The solution was diluted with benzene (10 mL), washed with H_2O (20 mL) and 1 N aqueous HCl solution (20 mL), and then dried over anhydrous magnesium sulfate. The solution was then filtered and concentrated in vacuo to a volume of ~2 mL. The concentrate was then passed through a column of silica gel with 1:1 hexanes/diethyl ether as eluent. Appropriate fractions from the column were combined and evaporated in vacuo, yielding 1 as a white crystalline compound (0.301 g, 70.4%; mp 106–108 °C). ^{1}H NMR δ 8.53 (d, J = 8.6 Hz, 1 H, H_c), 8.27 (d, J = 8.7 Hz, 1 H, H_d), 8.26 (d, J = 7.2 Hz, 1 H, $H_{c'}$), 7.56 (dd, J = 7.4 Hz, 1 H, H_b), 7.51 (dd, J = 8.4 Hz, 1 H, $H_{b'}$), 7.20 (d, J = 8.1 Hz, 2 H, PhH), 7.19 (d, J = 6.6 Hz, 1 H, H_a), 7.01 (d, J = 8.1 Hz, 2 H, PhH), 6.61 (dd, J = 10.8, 17.6 Hz, 1 H, CH=), 5.66 (d, J = 17.6 Hz, 1 H, =CH), 5.21 (d, J = 10.8 Hz, =CH), 4.83 (br t, J = 5.9

Table II
Bulk Polymerizations

	reaction mixtures						
polymer[a]	DVB, g	styrene, g	DIPB, g	AIBN, mg	toluene, mL	CH_3CN, mL	probe 1, 10^3 g
DVB-50-B-T	8.00	0	0	80	8	0	2.27
DVB-50-B-A	8.00	0	0	80	0	8	2.27
DIB-50-B-T	0	3.20	4.80	80	8	0	2.24
DIB-50-B-A	0	3.20	4.80	80	0	8	2.24

[a] Polymer code refers to cross-linking monomer (DIP = diisopropenylbenzene, DVB = divinylbenzene)-% cross-linker in monomer mixture-type of polymerization (B = bulk, S = suspension)-porogen (T = toluene, A = acetonitrile, N = no porogen).

Hz, 1 H, NHS), 4.05 (d, J = 6.0 Hz, 2 H, CH_2N), 2.90 (br s, 6 H, NMe_2); ^{13}C NMR δ 152.30, 137.36, 136.38, 135.84, 134.74, 130.78, 130.13, 129.83, 128.69, 128.55, 128.21, 126.49, 123.38, 118.81, 115.40, 114.37, 47.35, 45.65; IR ($CDCl_3$) 3390, 3160, 2950, 2260 (s), 1800, 1570, 1460, 1390, 1330, 1220, 1150, 900 (br), 760 (br), 710 (br), 650 cm^{-1}. High resolution MS calcd for $C_{21}H_{22}N_2O_2S$: 366.1404. Found: 366.1384.

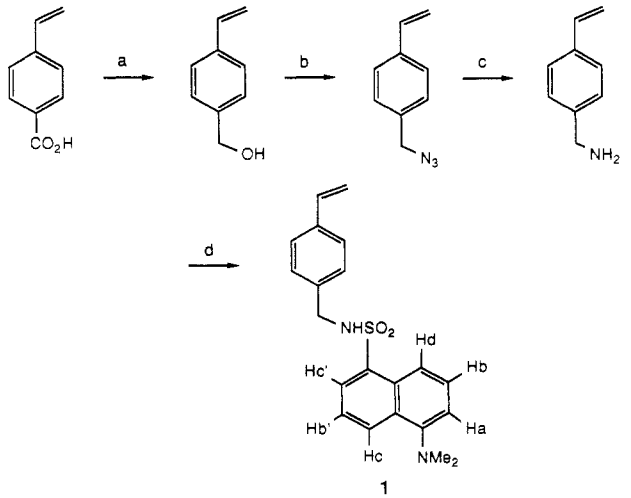

1

(a) $LiAlH_4$, Et_2O, reflux, 1.25 h; (b) MsCl, NEt_3, DMF, NaN_3, 0 °C–room temperatue, 10 h; (c) $LiAlH_4$, Et_2O, room temperature, 1 h; (d) dansyl chloride, benzene, NEt_3, 12 h.

Polymerizations. General. Styrene was obtained from Aldrich Chemical Co., divinyl benzene from MCB, and *m*-diisopropenylbenzene from the Goodyear Tire Co. These monomers were all washed twice with 10% aqueous sodium hydroxide solution and once with aqueous saturated sodium chloride solution (brine) and then dried over anhydrous magnesium sulfate prior to distillation. Divinylbenzene composition was determined by GC analysis.[10] AIBN was recrystallized from methanol and stored at −20 °C. Toluene and acetonitrile were distilled from calcium hydride and stored over molecular sieves (3 Å). Stock solutions of dansyl probe 1 in toluene or acetonitrile (concentration of 1 × 10^{-3} g of probe/mL of solvent) were prepared.

Suspension Polymerization. H_2O used was purified by filtering deionized water through a Nalgene millipore purification apparatus. Methocel K-100LV was obtained from Dow Chemical Co.

All suspension polymerizations were done in the same manner. The formulations differ with regard to the amount of cross-linking monomer and to the presence or absence of the diluent toluene. Preparations carried out were highly reproducible. A typical reaction is as follows (Table I):

A 500-mL three-neck (24/40, 45/50, 24/40) Morton flask was fitted with a Teflon stirrer bearing that supported an 18-in. stainless steel shaft with a 1 $^3/_4$-in. propeller attached on one end. The side necks contained a water cooled condenser and a stopper. The stainless steel stirrer was positioned so that the propeller lay submerged approximately one-third the distance from the top of the total liquid volume in the reaction mixture. The steel shaft was driven by a Lightnin' stirrer at a rotational speed of approximately 1000 rpm. The apparatus was sufficiently gas tight so that a constant N_2 atmosphere could be maintained throughout the reaction.

The Methocel dispersant (100 mg) was poured into 80–90 °C H_2O (50 mL) and the solution stirred to effect dispersion of the cellulose. The solution was allowed to cool to room temperature, at which time the dispersion became homogenous; the solution was added to the Morton flask and diluted with room-temperature H_2O (150 mL). The solution was then agitated by stirring for 15 min to ensure homogeneity. Technical grade divinylbenzene (20.0 g, 50% divinylbenzene isomers, 43% ethylvinylbenzene isomers, and 7% styrene) was added to the reaction vessel along with dansyl probe (5.66 × 10^{-3} g, 15.5 μmol) in toluene (20.0 mL) and AIBN (200 mg). The reaction mixture was degassed for 5 min by bubbling N_2 gas through the stirred solution via a stainless steel needle. The needle was then removed, the neck stoppered, and N_2 gas purged into the system through the condenser. With stirring, the suspension was brought to 70 °C and maintained for approximately 8 h.

After reaction, the suspension was filtered through a 75-μm screen and washed with spectral grade acetone. The beads were air dried and then were poured into a 250-mL round-bottom flask and refluxed with spectral grade acetone (150 mL) for 6 h. The beads were again screened at 75 μm and washed liberally with spectral grade acetone to remove any remaining Methocel and unreacted monomer. They were then dried under high vacuum for at least 6 h. The beads were then sifted, and the appropriate size was retained.

Bulk Polymerization. A typical bulk polymerization was performed as follows:

All components of a given polymerization (Table II) were placed in a 35-mL-capacity medium-walled tube that had one end closed off and the other constricted for sealing. The solution was freeze–thaw–degassed (3×), frozen once more, and sealed. The tube was allowed to warm to room temperature before being put into an oil bath adjusted to the desired polymerization temperature.

The polymer obtained was gently ground with mortar and pestle, and the 75–250-μm particle size was collected and Soxhlet extracted with spectral grade acetone for 12 h. The polymers were then vacuum dried for 6 h and sieved for the appropriate size.

Synthesis of Linear Polystyrene (LPS). Anionic polymerization[11] utilizing sodium naphthalide as initiator was employed to synthesize a copolymer of styrene and probe 1. The initiator was prepared by stirring, with a glass-coated magnetic bar, 1.5 g (11.7 mmol) of naphthalene and 1.5 g (65.2 mmol) of sodium metal in 50 mL of tetrahydrofuran for 2 h. The polymerization was carried out in a 100-mL Schlenk flask (with sidearm) equipped with a magnetic stir bar. After drying overnight in an oven, the hot flask was stoppered with two septa, and the stopcock in the sidearm was closed. A drying tube was connected to the main neck of the flask, the stopcock to the sidearm was opened, and the flask was purged with nitrogen for 15 min. With nitrogen flowing, tetrahydrofuran (49.0 mL), styrene (5.0 mL, 43.6 mmol), and 1 (1.00 mL of a 1.60 × 10^{-3} g/mL stock solution in tetrahydrofuran, 4.37 × 10^{-3} mmol) were syringed in. The drying tube was removed, and the nitrogen pressure was increased. The flask was cooled to −78 °C and allowed to thermally equilibrate for 5 min. While stirring, 1.0 mL of the green sodium napthalide solution was syringed quickly into the reaction flask. A deep red color was formed immediately and remained throughout the polymerization. After 5 min, the polymerization was quenched by addition of 2.0 mL of methanol. The clear solution was allowed to warm to room temperature. Methanol (30 mL) was then added to precipitate the polymer. The polymer was filtered, washed thoroughly with methanol, and dried in vacuo. The solid was crushed gently in a mortar and the fine powder was Soxhlet extracted for 1 day with methanol. The polymer thus obtained

Table III
Polymer Swelling and Template Hydrolysis Yields

polymer	% vol increase			hydrolysis % yield	
	toluene	MeOH	THF	MeOH	THF
	Suspension Polymers				
DVB-50-S-T	65				
DVB-50-S-N	15				
DVB-20-S-T	70				
DVB-20-S-N	30				
DVB-5-S-T	600				
DVB-5-S-N	100				
	Bulk Polymers				
DVB-50-B-T	50	25	30	64	20
DVB-50-B-A	5	10	5	14	0
DIB-50-B-T	140	5	140	41	94
DIB-50-B-A	40	15	40	84	30

was dried under high vacuum (10^{-4} mmHg) overnight to yield 4.50 g (99%) of doped polystyrene. DP (calc) = 372; M_w = 38 800; 1 probe/27 chains. GPC analysis was obtained on a Waters GPC I with two linear Ultrastyragel columns at 40 °C with toluene as solvent (RI detection; 1.0 mL/min flow rate). $\bar{M}_w$ = 42 090; $\bar{M}_n$ = 16 451; $\bar{M}_w/\bar{M}_n$ = 2.56.

Fluorescence Measurements. Emission and excitation spectra were recorded on a Hitachi Perkin-Elmer MPF-2A fluorescence spectrophotometer. All solvents were spectral grade (Aldrich) and used without further purification. Into a quartz, dual-path-length microcuvette (10 mm × 2 mm) was placed 50 mg of polymer (125–150 μm, if cross-linked) and 0.50 mL of solvent. The cuvette was capped, shaken, and allowed to stand for at least 30 min. Excitation and emission spectra were then recorded. These spectra were identical with those of polymers which were allowed to soak for 1 day. Cross-linked polymers were insoluble in all solvents, and the cuvette was aligned so that the light beam passed through the submerged polymer layer. Due to the broadness of the emission curve for the dansyl probe, the error in determining λ^{fl}_{max} was ±2 nm.

Solvent Swelling. Dry polymer (1 cm^3) was placed and tapped down in a 5-mL graduated cylinder that was calibrated at each tenth of a centimeter. Particles of 150–250 μm were used in all cases. Excess solvent was added to solvate the polymers. The polymer was stirred to permit escape of trapped air bubbles and to allow complete solvation of the particles. The particles were then packed down by vibrating and tapping down on the cylinder until no further settling was noted. Swelling equilibration occurs in a matter of approximately 4 h; however, measurements were taken after 24 h to ensure equilibration. The results are summarized in Table III.

Template Hydrolysis Procedure. Network copolymer (500 mg, 75–250-μm particle size), containing 1 mol % bisketal template assembly (**2**),[12] was placed into a 25-mL round-bottom flask containing methanol (10 mL) and 10% aqueous H_2SO_4 (1 mL). The mixture was stirred at reflux under a N_2 atmosphere for approximately 24 h. After this time, the heat source was removed and the condenser rinsed with a few milliliters of hot methanol. The suspension was then filtered through a sintered glass funnel and rinsed with hot methanol (20 mL) and then hot benzene (3 × 15 mL). The filtrate was then evaporated in vacuo to a concentrated solution of volume of 5 mL.

The concentrate was then diluted with benzene (25 mL) and extracted with brine (15 mL), aqueous saturated sodium bicarbonate solution ($NaHCO_3$, 15 mL), and then again with brine (15 mL). The organic layer was dried with potassium carbonate, and an internal standard was added. The solution was allowed to stand for ~20 min and then gravity filtered and concentrated to 2 mL. GC analysis was performed on the concentrate. All manipulations were carried out so as to ensure quantitative transfer. An analogous procedure was used for hydrolyses carried out in THF.

Results and Discussion

The utility of the dansyl group as an environmental probe originates from the wavelength dependence of its fluorescence emission which varies as a function of solvent (microenvironment).[13] A summary of λ^{fl}_{max} of probe **1** in various solvents is given in Table IV. To best evaluate how a polymer matrix perturbs the microenvironment of the probe, a graphical presentation of λ^{fl}_{max} versus solvent property was desired. The empirical solvent treatment of Taft and Kamlet[14,15] was used to generate eq 1 which

$$\lambda^{fl}_{cal}\ (nm) = 53.45\pi^* + 20.48\alpha + 9.932\beta + 457.1 \quad (1)$$

permits calculation of the fluorescence emission of probe **1** in any solvent with known values of π^* (solvent dipolarity/polarizability), α (hydrogen bond donor strength), β (hydrogen bond acceptor strength).[14] The fluorescence emission over a range of pure solvents exhibits a reasonable correlation (r = 0.98), and a plot of λ^{fl}_{cal} versus λ^{fl}_{exp} is given in Figure 1. The diagonal correlation line forms a reference for the fluorescence emission of probe **1** in pure organic solvent.

Table IV
Fluorescence Emission Maximum of Probe 1

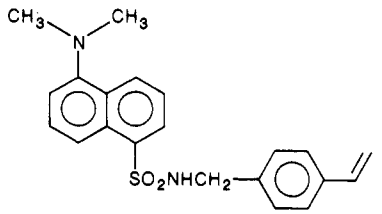

λ_{max}	solvent	λ_{max}	solvent
454	hexane	512	ethanol
473	ether	517	acetonitrile
485	dioxane	519	methanol
492	ethyl acetate	520	DMSO
504	acetone	538	water
510	DMF		

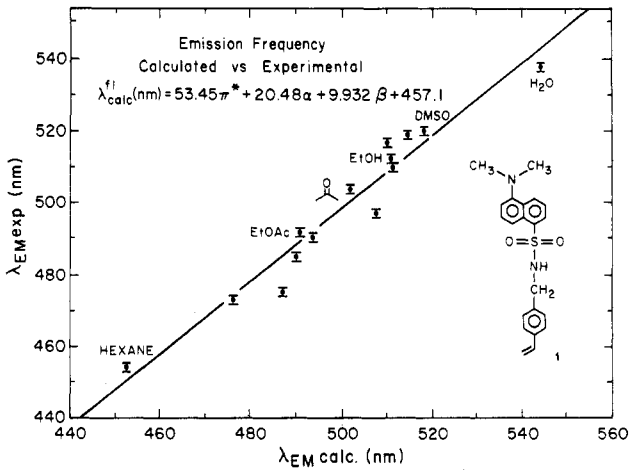

Figure 1. Plot of calculated versus experimental fluorescence emission of dansyl probe **1** in pure organic solvents.

Analysis of the Solvatochromic Shift: Linear Polystyrene. The fluorescence emission of probe **1** doped in *dry* linear polystyrene (LPS) prepared by anionic polymerization is 459 nm. A plot of λ^{fl}_{exp} of dilute solutions (0.0028 M) of doped LPS in various solvents is included in Figure 2. Two benchmarks are included in the plot, the fluorescence emission of probe **1** in pure organic solvents and the fluorescence emission of dry polystyrene (cross-hatching). Of special note is the observation that the fluorescence emission of LPS in may solvents parallels the pure solvent correlation line, suggesting extensive polymer chain solvation in solvating media up to and including CH_2Cl_2. A dramatic blueshift is noted upon going from CH_2Cl_2 to EtOH; indeed the λ^{fl}_{exp} in EtOH resembles that of *dry polymer*. Since EtOH is a *nonsolvent* for LPS,

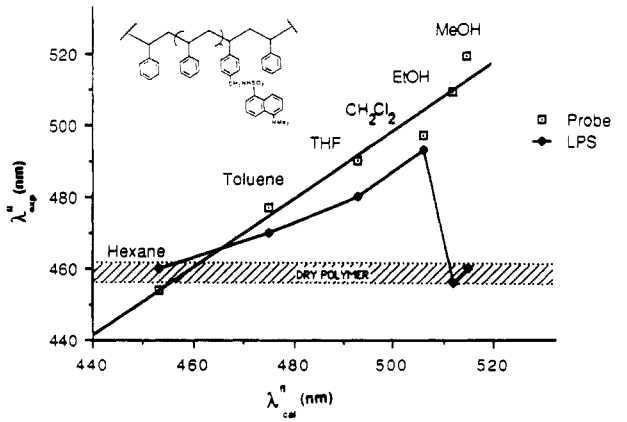

Figure 2. Fluorescence emission of solvent equilibrated LPS doped with dansyl probe 1.

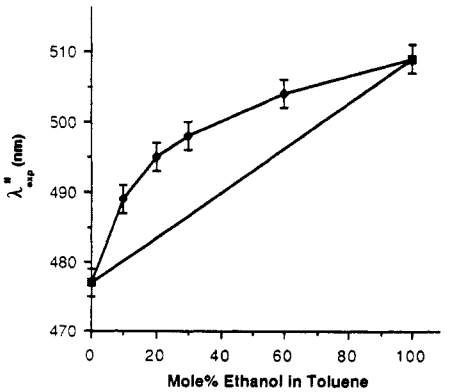

Figure 3. Plot of fluorescence emission of probe 1 in the solvent pair ethanol–toluene (mole percent). (●) Experimental points. The tie line represents an ideal linear relationship.

the fluorescence emission reveals a solvent-excluded precipitated polymer particle. The principle determinant in providing the microenvironment of the probe is the polymer backbone. The *degree* to which λ^{fl}_{exp} parallels either the pure solvent correlation line or the dry polymer regime permits a *qualitative* comparison of materials with regard to their penetrability toward various solvents.

The proximity of the fluorescence emission wavelength of solvent-imbibed polymers to the emission in pure solvents is useful for qualitative comparisons but should not be used as a quantitative measure of the extent of solvation. This caveat is necessary since the polymer–solvent system represents a mixed solvent system in which a breakdown in a linear correlation is noted. For example, plots of λ^{fl}_{exp} for probe 1 in toluene–ethanol are not linear with respect to the mole fraction of solvent (Figure 3). The degree to which the linear relationship between mole fraction of solvent in a mixed solvent system and the solvatochromic shift breaks down is solvent dependent. For example, a far better linear correlation is found for the toluene/CH_2Cl_2 solvent pair (Figure 4). It is likely, therefore, that the origin of this deviation resides in specific strong solute (probe)–solvent interactions since the poorest linear correlations occur with solvents that can act as hydrogen bond donors or acceptors.

The preceding provides the basis for interpreting the solvent dependence of the wavelength of fluorescence emission of probe 1 in networks of styrene–divinylbenzene (ST–DVB) and styrene–diisopropenylbenzene (ST–DIB).

Solvent Penetrability versus Degree of Cross-Linking: Nonporous ST–DVB "Glassy Beads". A series of nonporous ST–DVB copolymers ranging from 5% to 50% cross-linking were prepared by suspension polymerization. The molar ratio of probe 1 to total monomers

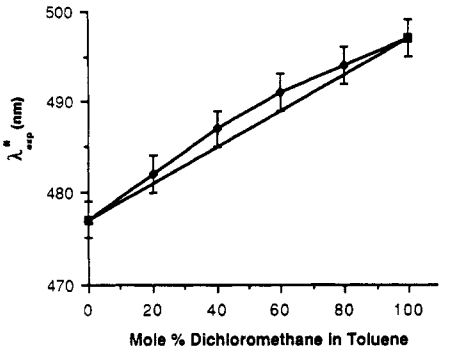

Figure 4. Plot of fluorescence emission of probe 1 in the solvent pair CH_2Cl_2–toluene (mole percent). (●) Experimental points. The tie line represents an ideal linear relationship.

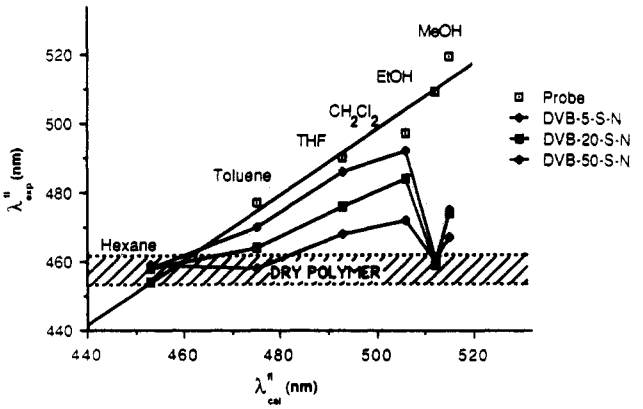

Figure 5. Fluorescence emission of solvent-equilibrated "glassy beads" doped with dansyl probe 1.

was 10^{-4}. The transparent nonporous spheres were sized, and a cut spanning the range 125–150 μm was used for study. The fluorescence emission of dry beads was recorded then the beads were soaked in the indicated solvent. The fluorescence emission of solvent-swollen beads were recorded in a quartz microsampling cell, and the results are summarized in Figure 5.

The fluorescence emission of solvent-equilibrated "glassy beads" displays a trend which parallels the cross-link percentage (Figure 5). The 50% cross-linked beads (DVB-50-S-N) parallel the "dry" polymer correlation line, indicating relatively little probe solvation. However, as cross-linking is decreased, the extent of solvation increases, as evidenced by the progressively closer parallel to the pure solvent correlation line. Thus, probe 1 readily reveals that these nonporous gels are solvated to an extent which is controlled by the degree of cross-linking. A departure from this trend is noted in poor swelling solvents (EtOH) where *all* polymers exhibit fluorescence emission that approximates the dry state (no solvation), a situation that indicates the networks remain collapsed and the polymer backbone dominates the probe microenvironment. Interestingly, *all* polymers exhibit a blue shift upon changing from CH_2Cl_2 to EtOH. This finding indicates that *all* polymers surveyed, even DVB-50-S-N, are solvated to some degree in good swelling solvents (i.e., CH_2Cl_2).

The fluorescence emission maxima represent an average of the microenvironments of probe molecules in the polymer network. The relationship between these values and the *macroscopic* properties of the polymer particles, such as volume increase, may be evaluated from the data in Table III.

The volume increase is influenced by the degree of cross-linking *and* by the nature of the solvent. The observed trend in this series is consistent with what is known regarding solvation of network polymers. An increase in

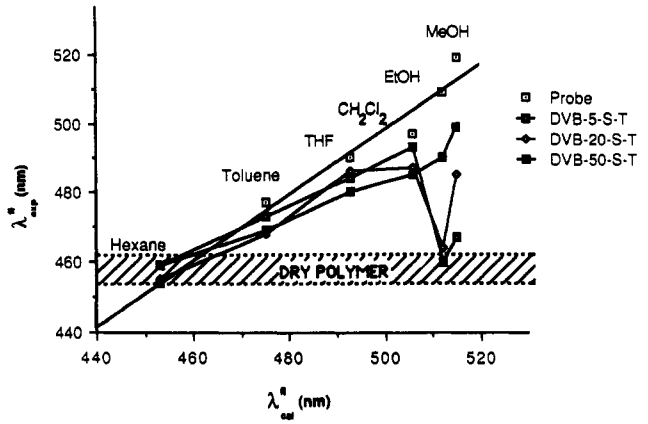

Figure 6. Fluorescence emission of solvent equilibrated macroporous styrene–divinylbenzene copolymers doped with probe 1 and prepared by suspension polymerization.

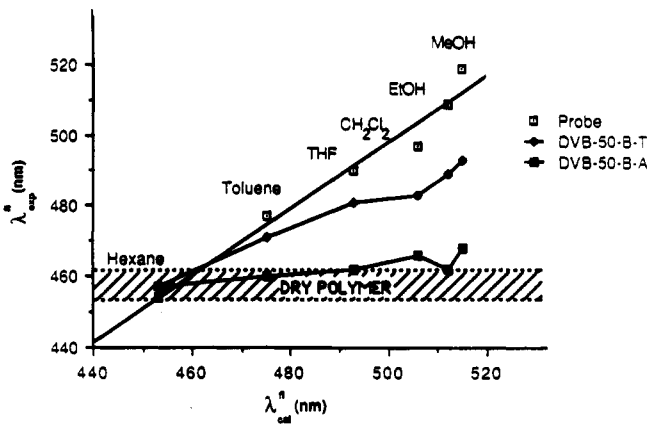

Figure 7. Fluorescence emission of solvent-equilibrated macroporous divinylbenzene copolymers doped with probe 1 and prepared by bulk polymerization.

cross-linking diminishes the solvent-induced volume increase, while at constant cross-linking the polymer volume increase parallels the solvating ability of the solvent.[16] Importantly, the qualitative correspondence between these data and the solvatochromic data provide the key link between fluorescence emission and gel-phase solvation.

Macroporous Styrene–Divinylbenzene Copolymers: Influence of Morphology and Cross-Linking on Gel Solvation. To evaluate the utility of the probe technique for the analysis of more complex materials such as macroporous polymers, a series of DVB copolymers (e.g., DVB-50-S-T) were prepared by suspension polymerization using toluene as porogen (Table I). The volume of porogen to monomer was held constant (volume of solvent/(volume of solvent + volume of monomer), f_m = 0.5) while the percent cross-linking was varied from 5% to 50%. The influence of porogen in the polymerization reaction on solvent penetrability is readily apparent upon consideration of Figure 6. Unlike the nonporous gels, all polymers prepared by suspension polymerization with toluene as porogen exhibit fluorescence emission that strongly parallels the pure solvent correlation line (Figure 6). This finding indicates a substantial degree of probe solvation. Indeed, even the 50% cross-linked material (DVB-50-S-T) exhibits solvation behavior similar to more lightly cross-linked 5% glassy beads (DVB-5-S-N, Figure 5). An important difference in this series occurs in the poor swelling solvents (EtOH). In this solvent, the 5% and 20% cross-linked materials (DVB-5-S-T, DVB-20-S-T) exhibit a fluorescence emission that parallels the "dry" polymer, a consequence of a collapsed network structure. *However, the emission of 50% cross-linked material (DVB-50-S-T) remains close to the pure solvent correlation line.* This observation reveals a truly permanent *micropore*[4a,19b,20b] structure that remains intact, regardless of solvent. Thus, even the highly polar solvent EtOH can penetrate and solvate the probe in 50% cross-linked macroporous materials (DVB-50-S-T).

Macroporous Divinylbenzene Polymers: Influence of Porogen and Polymerization Type on Gel Solvation. Two macroporous polymers were prepared by bulk polymerization from technical grade divinylbenzene. although these materials have the same nominal degree of cross-linking (50%), they differ in the porogen employed. In one, a solvating porogen (toluene; DVB-50-B-T) was employed, and in the second, a nonsolvating porogen (acetonitrile; DVB-50-B-A) was employed (f_m = 0.5) (Table II).[17] Characterization of these materials included analysis of the pore structure in the dry state by N_2 adsorption and Hg penetration porosimetry. A summary of these data is given in Table V. The λ^{fl}_{exp} of these polymer particles soaked in various pure organic solvents is given in Figure 7.

Table V
Comparison of Macroreticular Divinylbenzene and Diisopropenylbenzene–Styrene Copolymers

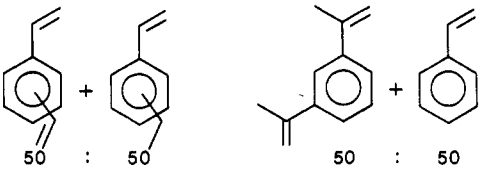

	diluent		
	acetonitrile	toluene	toluene
residual double bonds, %	11.6	9.8	25.0
surface area, m^2/g			
N_2	215	407	598
Hg	116	0.8	85
av pore radius, Å			
N_2	91	19	557
Hg (50% vol)	350	800	650
pore vol (N_2), cm^3/g	0.98 (<1300 Å)	0.396 (<1300 Å)	1.66 (>1300 Å)

With toluene as diluent (DVB-50-B-T), solvent-dependent fluorescence emission reveals the highly cross-linked network closely parallels the pure solvent correlation line, indicating the probe is highly solvated even in poor solvents for linear polystyrene (Figure 7). This result indicates a polymer gel phase with a high degree of permanent *micropore* structure. We have found no difference between this material and that prepared by suspension polymerization (DVB-50-S-T).

Quite interestingly, when the bulk polymerization is run with CH_3CN as diluent, the resulting polymer does *not* parallel the solvent correlation line; rather it parallels very closely the "dry" polymer region, indicating very little solvation in all solvents. This implies these materials are comprised of a gel phase that is *substantially* less pervious to all solvents. Although differences in physical and chemical properties between macroporous materials prepared with solvating and nonsolvating porogens have been noted by a number of investigations,[18-20] the probe method affords a decisive comparison of these materials with regard to solvent penetrability.

Materials prepared with the two porogens have different morphologies in the dry state. For example, the distribution of pores in material prepared with toluene as porogen is weighted toward small micropores when compared

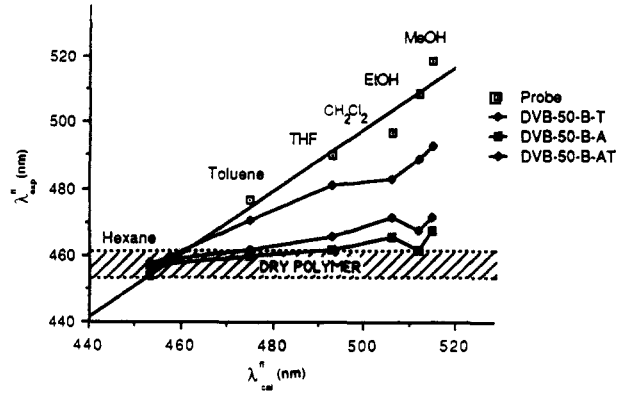

Figure 8. Fluorescence emission of DVB-50-B-A soaked in CH_3CN for 2 weeks (labeled DVB-50-B-AT). For reference, plots of DVB-50-B-A and DVB-50-B-T equilibrated for 1 day are included.

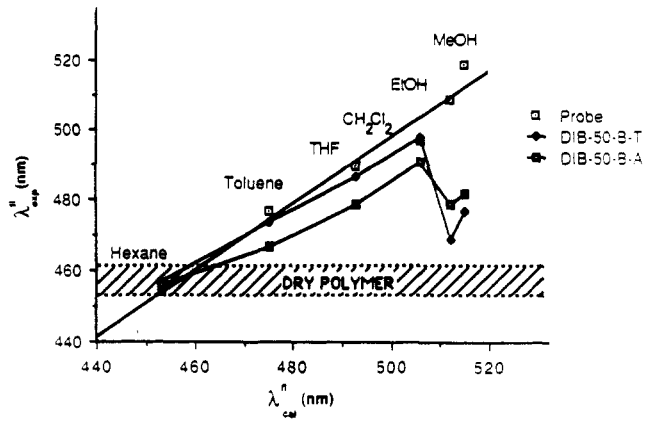

Figure 9. Fluorescence emission of solvent-equilibrated macroporous styrene–diisopropenylbenzene copolymers doped with probe 1.

with material prepared with CH_3CN as porogen. It is important to note that in most cases swelling (but not solvent uptake) is a valuable predictor. However, no single property, i.e., swelling, pore size, or surface area, provides a completely reliable guide regarding solvent penetration of the polymer matrix.

The origin of the differences between the two materials arises from the differences in the solvating ability of the two porogens and not from factors such as chain-transfer differences between the two solvents.[21-23] In good polymer solvents, the phase separation can produce a solvent-swollen gel phase, while in poor polymer solvents (CH_3CN) a collapsed structure may be formed. The solvent-swollen gel phase results in an expanded network that remains penetrable to all solvent molecules.

The collapsed network produced upon polymerization with nonsolvent porogens may be solvent modified by long-term exposure to swelling solvents.[24] Figure 8 plots the solvatochromic shift of DVB-50-B-AT, a solvent-modified polymer of DVB-50-B-A, that has been soaked in toluene for 2 weeks. For reference, the solvatochromic shifts of DVB-50-B-A and DVB-50-B-T are also included. It is clear that prolonged soaking of these polymer networks produces changes in their penetrability toward solvents; for example, the solvent-modified DVB-50-B-AT exhibits fluorescence properties that approach DVB-50-B-T. Similarly, long-term soaking in acetonitrile of DVB-50-B-T results in a material whose fluorescence behavior approaches that of DVB-50-B-A.

The results of the present study reveal two time domains with regard to solvent penetration of networks. One is of a short duration (minutes to days) where no significant changes in swelling or fluorescence emission are noted. The long-term experiments ($\sim^1/_2$ month) reveal a slower process resulting in network reorganization that produces changes in solvent penetrability. These long-term experiments do not necessarily imply an equilibrium state is achieved.

Macroporous Diisopropenylbenzene–Styrene Copolymers: Influence of Cross-Linking Monomer. Two macroporous polymers were prepared by bulk polymerization of 1:1 mixtures of diisopropenylbenzene–styrene.[25,26] Solvating (toluene) and nonsolvating porogens (CH_3CN) were used. The solvatochromic results are presented in Figure 9. One notes that the differences that arise from the nature of the porogen for these materials is less dramatic than for DVB networks. Significant differences do emerge, however, upon comparing DVB and DIB networks. Although both contain the same nominal degree of cross-linking (50%), the DIB networks reveal a more complex behavior upon changing from good polymer solvents to nonsolvents. The blue shifts that are observed in both DIB-50-B-A and DIB-50-B-T in ethanol and methanol reveal that these networks are considerably more flexible than those prepared with DVB and respond in significant ways to changes in the solvating power of the solvent. In good swelling solvents, the networks are expanded and highly solvated and in poor solvents the networks are collapsed and have very limited accessibility to solvents. These differences are more pronounced in DIB-50-B-T than in DIB-50-B-A. In contrast, DVB-50-B-T remains expanded and previous to *all* solvents regardless of their solvating ability.

The origin of the differences between DVB and DIB networks arises *in part* from the fact that fewer double bonds have been incorporated into the DIB network, resulting in lower effective cross-linking density (Table V).[26] Swelling studies in toluene are also consistent with these results; the DIB-50-B-T network more than doubles its size in toluene, whereas DVB-50-B-T swells to a lesser degree. It should be noted, however, that the nature of the porogen exerts a significant influence on the degree of swelling of these materials, compare, for example, the last two entries in Table III.

Bisketal Hydrolysis: Relationship between the Solvatochromic Results and Chemical Reactions in the Gel Phase. The solvatochromic shift studies reveal significant differences between amorphous networks regarding solvent penetrability. We desired to evaluate the utility of this information by comparing these results with a study of the hydrolysis of bisketal templates that have been covalently incorporated into the gel phase. A series of network polymers were prepared incorporating a bisketal template assembly via copolymerization.[12] The materials were prepared in an identical manner with materials used in the solvatochromic studies. Each polymer was subjected to three sequential 24-h hydrolysis cycles and the amount of 1,3-diacetylbenzene liberated from each hydrolysis was recorded. The results are summarized in Figures 10 and 11 (Table III).

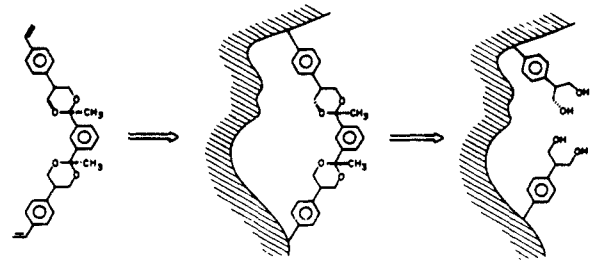

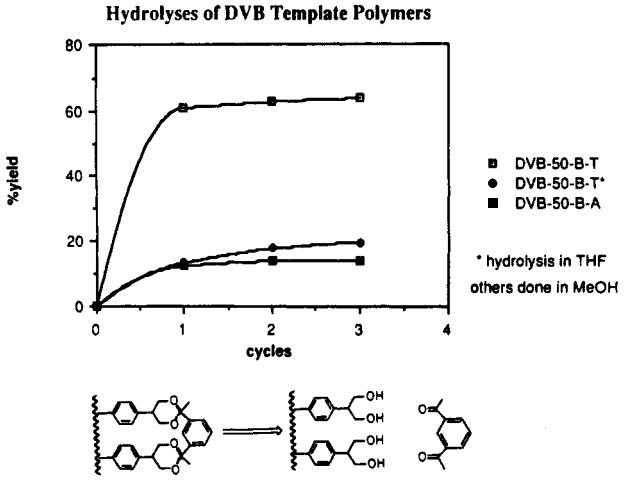

Figure 10. Hydrolysis yield of 1,3-diacetylbenzene from DVB template polymers. Each cycle represents a 24-h hydrolysis in the indicated solvent system. Note: hydrolysis of DVB-50-B-A in THF/H_2SO_4 gave no 1,3-diacetylbenzene.

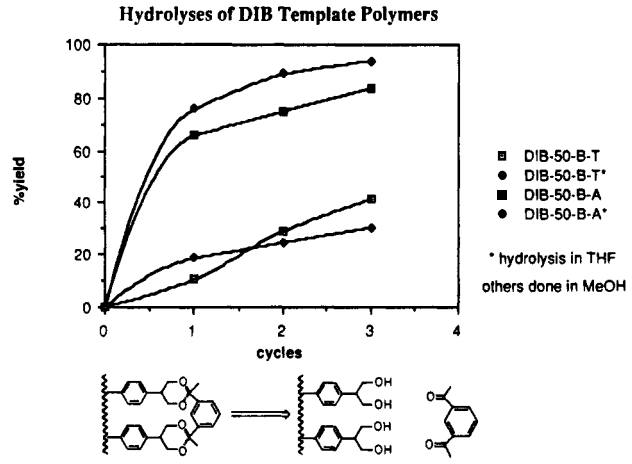

Figure 11. Hydrolysis yield of 1,3-diacetylbenzene from DIB template polymers. Each cycle represents 24-h hydrolysis in the indicated solvent system.

There is a striking difference in the hydrolysis yield for DVB polymers depending upon the porogen used for polymerization. With material prepared with toluene as porogen (DVB-50-B-T), approximately 60% of the total amount of 1,3-diacetylbenzene is liberated after one hydrolysis cycle with CH_3OH–H_2SO_4. Less than 15% 1,3-diacetylbenzene is obtained from hydrolysis of material prepared with CH_3CN as porogen (DVB-50-B-A). Importantly, this finding correlates with the solvatochromic results, i.e., the solvating porogen produces a polymer with a more solvent-accessible network than one made with a nonsolvating porogen (Figure 7). The correspondence between the solvatochromic shift results and our hydrolysis experiments permits us to utilize the fluorescence probe technique to survey complex materials with regard to their suitability as matrices in our template polymerization program.[12]

Solvent effects are also noted for the hydrolysis reaction of 1,3-diacetylbenzene templates from the DVB polymers. The "best" solvent system, that which yields the greatest amount of 1,3-diacetylbenzene in the shortest time, is $MeOH/H_2SO_4$. Over the same time period, hydrolysis yields are significantly lower for the THF/H_2SO_4 solvent system. This result parallels the hydrolysis rates of monomeric *bisketal* in *homogeneous solution* (k_{MeOH}/k_{THF} = 100).[27] The implication is that these macroporous DVB matrices provide a neutral environment that does not temper normal solvent effects on the hydrolysis reaction. The high penetrability of diverse solvents such as THF and MeOH in DVB-50-B-T, as revealed by the solvatochromic shift results (Figure 7), offers a clear prediction of this hydrolysis behavior.

More complicated behavior is exhibited for the DIB copolymers. For example, the solvatochromic shift results for DIB-50-B-T reveal the matrix accommodates good solvents (THF). The blue shift found in poor swelling solvents (MeOH), on the other hand, reveals a collapsed, solvent-excluded network. The hydrolysis results (Table III) show the best hydrolysis solvent is THF (contrary to that observed for DVB-50-B-T). On the other hand, the solvatochromic results for DIB-50-B-A reveal a diminished solvent-induced matrix effect. Interestingly, the $MeOH/H_2SO_4$ solvent system proves to be "best" for hydrolysis reactions involving this matrix despite the swelling data. Although the origins of these porogen effects on the DIB copolymers are not known, the probe technique provides information that can be used to predict hydrolysis yields. The solvatochromic data provide a detailed analysis of the complex behavior of these materials. It should be noted that the swelling results in THF also paralleled the hydrolysis yields; that is, materials that exhibited the largest volume increase in THF also gave the highest hydrolysis yield. In methanol, no consistent relationship exists between the volume increase and hydrolysis yield.

In summary, the solvatochromic shift of network polymers doped with the dansyl probe is found to qualitatively correlate with solvation of the network. Predictable trends are noted with regard to cross-linking density and permanent porosity. Of particular importance is the opportunity to identify subtle differences in the gel phase that arise during polymerization. These differences can result in a striking disparity of the network with regard to solvent penetrability. This behavior may otherwise be difficult to identify on the basis of the usual criteria used to characterize complex amorphous materials.

In a related paper,[7] the solvatochromic behavior is also found to correlate with the relative rates of diffusion of electrophilic reagents through these networks.

Acknowledgment. We thank the National Science Foundation for financial support of this work and IBM for a fellowship (to G.J.S.). We also thank Dr. Evan Thompson for assistance with the GPC analysis, the Goodyear Corporation for a generous sample of *m*-diisopropenylbenzene, and Dow Corning Corporation for the Methocel K100-LV.

Registry No. 1, 105029-42-3; (1)(styrene) (copolymer), 105186-78-5; (1)(styrene)(DIPB) (copolymer), 118018-24-9; (1)(styrene)(DVB) (copolymer), 105186-79-6; (1)(DVB) (copolymer), 117317-01-8; 2, 111020-03-2; *p*-vinylbenzyl alcohol, 1074-61-9; *p*-vinylbenzoic acid, 1075-49-6; *p*-vinylbenzyl acide, 111965-73-2; sodium azide, 26628-22-8; *p*-vinylbenzylamine, 50325-49-0; dansyl chloride, 605-65-2.

References and Notes

(1) Candau, S.; Bastide, J.; Delsanti, M. *Adv. Polym. Sci.* **1982**, *44*, 27.
(2) Rebenfeld, L.; Markarewicz, P. J.; Weigmann, H. D.; Wilkes, G. L. *J. Macromol. Sci., Rev. Macromol. Chem.* **1976**, *C15*, 279.
(3) see, for example: (a) Harrison, D. J. P. *J. Macromol. Sci., Rev. Macromol. Chem. Phys.* **1985**, *C25*, 481. (b) Horie, K.; Mita, I.; Kawabata, J.; Nakahama, S.; Hirao, A.; Yamazaki, N. *Polym. J. (Tokyo)* **1980**, *12*, 319. (c) Pickup, S.; Blum, F. D.; Ford, W. T.; Periyasamy, M. *J. Am. Chem. Soc.* **1986**, *108*, 3987. (d) Pan, S.-S. Morawetz, H. *Macromolecules* **1980**, *13*, 1157. (e) Ford, W. T.; Periyasamy, M.; Spivey, H. O. *Macro-*

molecules 1984, 17, 2881. (f) Gordon, J. E. J. Phys. Chem. 1962, 66, 1150. (g) Mikes, F.; Strop, P.; Tuzar, Z.; Labsky, J.; Kalal, J. Macromolecules 1981, 14, 175. (h) Strop, P.; Mikes, F.; Kalal, J. J. Phys. Chem. 1976, 80, 694.
(4) (a) Guyot, A.; Bartholin, M. Prog. Polym. Sci. 1982, 8, 277. (b) Heitz, W. Adv. Polym. Sci. 1977, 23, 1. (c) Funke, W. Chimia 1968, 22, 111. (d) Sherrington, D. C. In Polymer-Supported Reactions in Organic Synthesis, Hodge, P., Sherrington, D. C., Eds.; Wiley: New York, 1980; Chapter 1.
(5) (a) Beavan, S. W.; Hargreaves, J. S.; Phillips, D. Adv. Photochem. 1979, 11, 207. (b) Chapoy, L. L.; DuPré, D. B.; Biddle, D. Dev. Polym. Charact. 1986, 223. (c) Tanizawa, K.; Kanaoka, Y.; Lawson, W. B. Acc. Chem. Res. 1987, 20, 337. (d) Weber, G. Biochem. J. 1952, 51, 155. (e) Himel, C. M.; Mayer, R. T.; Cook, L. L. J. Polym. Sci., Polym. Chem. Ed. 1970, 8, 2219.
(6) (a) Shea, K. J.; Stoddard, G. J.; Sasaki, D. Y. Polym. Prepr. (Am. Chem. Soc., Div. Polym. Chem.) 1986, 27(2), 344. (b) Shea, K. J.; Okahata, Y.; Dougherty, T. K. Macromolecules 1984, 17, 296. (c) Shea, K. J.; Sasaki, D. Y.; Stoddard, G. J. Polym. Prepr. (Am. Chem. Soc., Div. Polym. Chem.) 1987, 28(2), 88. (d) Shea, K. J.; Stoddard, G. J.; Sasaki, D. Y. ACS Symp. Ser. 1987, No. 358, Chapter 9.
(7) Shea, K. J.; Stoddard, G. J.; Sasaki, D. Y., submitted for publication in Macromolecules.
(8) Leebrick, J. R.; Ramsden, H. E. J. Org. Chem. 1958, 23, 935.
(9) Mendel, A. J. Chem. Eng. Data 1970, 15, 340.
(10) Blasius, E.; Lohde, H. Talanta 1966, 13, 701.
(11) Collins, E. A.; Bares, J.; Billmeyer, F. W., Jr. Experiments in Polymer Science; Wiley-Interscience: New York, 1973; p 357.
(12) Shea, K. J.; Dougherty, T. K. J. Am. Chem. Soc. 1986, 108, 1091.
(13) (a) Li, Y.-H.; Chan., L.-M.; Tyer, L.; Moody, R. T.; Himel, C. M.; Hercules, D. M. J. Am. Chem. Soc. 1975, 97, 3118. (b) Chen, R. F. Arch. Biochem. Biophys. 1967, 120, 609. (c) Chen, H.-L.; Morawetz, H. Macromolecules 1982, 15, 1445. (d) Strauss, U. P.; Vesnaver, G. J. Phys. Chem. 1975, 79, 2426.
(14) Kamlet, M. J.; Abboud, J. L. M.; Taft, R. W. Prog. Phys. Org. Chem. 1981, 13, 485.
(15) Taft, R. W.; Abboud, J. L. M.; Kamlet, M.; Abraham, M. H. J. Solution Chem. 1985, 14, 153.
(16) Lloyd, W. G.; Alfrey, T., Jr. J. Polym. Sci. 1962, 62, 301.
(17) Millar, J. R. J. Polym. Sci., Polym. Symp. 1980, 68, 167.
(18) (a) Millar, J. R.; Smith, D. G.; Marr, W. E.; Kressman, R. E. J. Chem. Soc. 1963, 218. (b) Howard, G. J.; Midgley, C. A. J. Appl. Polym. Sci. 1981, 26, 3845.
(19) (a) Albright, R. L. React. Polym., Ion Exch., Sorbents 1986, 4, 155. (b) Sederel, W. L.; DeJong, G. J. J. Appl. Polym. Sci. 1973, 17, 2835.
(20) (a) Sherrington, D. C. Nouv. J. Chim. 1982, 6, 661. (b) Jacobelli, H.; Bartholin, M.; Guyot, A. Angew. Makromol. Chem. 1979, 80, 31.
(21) Mayo, F. R. J. Am. Chem. Soc. 1943, 65, 2324.
(22) Gregg, R. A.; Mayo, F. R. Discuss. Faraday Soc. 1947, 2, 328.
(23) Gregg, R. A.; Mayo, F. R. J. Am. Chem. Soc. 1953, 75, 3530.
(24) (a) Wieczorek, P. P.; Kolarz, B. N.; Galina, H. Angew. Makromol. Chem. 1984, 126, 39. (b) Kolarz, B. N.; Wieczorek, P. P.; Wojaczynka, M. Angew. Makromol. Chem. 1981, 96, 193.
(25) Colvin, H. A.; Muse, J. CHEMTECH 1986, 500.
(26) Hild, G.; Okasha, R. Makromol. Chem. 1985, 186, 389.
(27) Pseudo-first-order rate constants for the hydrolysis of monoketal i were determined spectrophotometrically.
(28) The pseudo-first-order rate constants in $MeOH/H_2SO_4$ and THF/H_2SO_4 are 3×10^{-3} and 6×10^{-5} s^{-1}, respectively.

Microstructural Evolution of a Silicon Oxide Phase in a Perfluorosulfonic Acid Ionomer by an in Situ Sol–Gel Reaction. 1. Infrared Spectroscopic Studies

K. A. Mauritz* and R. M. Warren

Department of Polymer Science, University of Southern Mississippi, Southern Station Box 10076, Hattiesburg, Mississippi 39406-0076. *Received July 6, 1988; Revised Manuscript Received October 4, 1988*

ABSTRACT: Unique microcomposite membranes have been produced via the sol–gel reaction for silicon tetraethoxide within the microphase morphology of hydrated perfluorosulfonic acid films. FT-IR spectroscopy has been used to monitor the aspects of molecular organization within the invasive gel as a function of silicon oxide content. We have assigned five of the major peaks to characteristic group vibrations based on an assessment of prior experimental infrared studies of various siloxanes, silicates, and silicas as well as theoretical vibrational analyses of these systems. Our spectral analysis depicts an evolving ≡Si—O— network that grows to become increasingly less interconnected but more strained. The broadness of the peaks suggests a gel microstructure that is considerably heterogeneous.

Introduction

In a recent report, Mauritz et al. outlined a simple method for producing unique microcomposite membranes by the in situ growth of a silicon oxide phase in hydrated perfluorosulfonic acid films (Nafion, E. I. du Pont de Nemours & Co.) via the acid-catalyzed sol–gel reaction for tetraethoxysilane (TEOS) that was allowed to diffuse into the films from external alcohol solutions.[1] After immersion in these solutions for prescribed times, the membranes were carefully dried/annealed to optimize the network connectivity of the incorporated gel component by condensation involving unreacted OH groups. Throughout these studies, our primary working hypothesis has been that the resultant morphology of the silicon oxide phase will be ordered by the prior established three-dimensional pattern of phase separation, having periodicity on the scale around 50 Å. It is in fact convenient, if not fortuitous, that small-angle X-ray scattering studies of acid-catalyzed silica produced via the sol–gel route yield a radius of gyration of 15–17 Å, i.e. silicate clusters having a natural size that is quite close to that of the Nafion polar clusters in which we expect them to grow.[2] We tend to exercise caution in referring to the in-growths as "silica gel" in the usual sense as we expect this microphase to be rather finely dispersed throughout the polymer matrix so as to possess a very high surface-to-volume ratio and have a comparatively high population of nonbridging oxygens and low degree of cyclization. Presently, therefore, we choose to use the term "silicon oxide", pending more definitive structural characterization.

The trend of mechanical tensile properties versus solids uptake includes a ductile-to-brittle transformation that

0024-9297/89/2222-1730$01.50/0